Time evolution of ion energy distributions and optical emission in pulsed inductively coupled radio frequency plasmas

Martin Misakian,[a] Eric Benck, and Yicheng Wang
National Institute of Standards and Technology, Gaithersburg, Maryland 20899-8113

(Received 12 April 2000; accepted for publication 26 July 2000)

This article reports the results of time-resolved measurements of ion energy distributions (IEDs), relative ion densities, as well as optical emissions and electrical characteristics in pulsed inductively coupled plasmas for the simple gas mixture of oxygen and argon (50%Ar:50%O_2). The peak radio frequency power, frequency, repetition rate, and duty cycle were 200 W, 13.56 MHz, 500 Hz, and 85%, respectively. Examination of the time evolution of the data over the pulse cycle indicates that when the plasma is energized, it begins in the dim (E) mode undergoing at first slow changes in certain plasma parameters. After about 1.2 ms, a sudden transition to the bright (H) mode occurs. The characteristics of the IEDs are consistent with an average plasma potential profile that has (a) a relatively large collisionless sheath and narrow presheath during the dim mode and (b) a very narrow sheath and greatly extended presheath during the bright mode; the ion mean free path influences the peak position of the IED during the bright mode. For most of the pulse cycle, the relative abundances of the ions Ar^+, O_2^+, and O^+ maintain the relation $\%O_2^+ \geq \%Ar^+ > \%O^+$. [S0021-8979(00)01621-2]

I. INTRODUCTION

The transition of inductively coupled rf plasmas from the dim or E mode with low light emission to the bright or H mode with intense light emission as power to an energizing coil is increased has been recognized for many years.[1–5] More recently, pulsed inductively coupled plasmas, which can undergo E- to H-mode transitions, have received considerable attention because of their possible advantages over continuous plasma discharges in industrial processes.[6–8] This article examines the time evolution of the plasma through time resolved recordings of the ion energy distributions (IEDs) at the grounded electrode of a Gaseous Electronics Conference (GEC) rf reference cell[9] that is modified to operate in an inductively coupled[10] pulsed mode.[11] The time resolved IED results provide some insights into the behavior of the average potential profile in the plasma during the two modes, which may have implications for determining the relative abundances of ions from measurements of IEDs. The results of concurrent measurements of optical emissions, coil current, and voltage wave forms, which have higher time resolution than the ion data, are also presented. The simple gas mixture of argon and oxygen is used for performing most of the measurements, but some comparisons are also made with data obtained using pure argon. Section II provides a brief description of the experimental arrangement and conditions, sec. III describes the experimental results, and Sec. IV discusses the results. A summary with some conclusions is given in Sec. V.

II. EXPERIMENTAL APPARATUS AND CONDITIONS

Plasmas were generated in a GEC rf reference reactor whose upper electrode was replaced with a five-turn planar rf-induction coil behind a quartz window to produce inductively coupled discharges.[10] The ion sampling arrangement is the same as that used to study inductively coupled plasmas generated in CF_4 under continuous excitation.[12] Ions are sampled through a 10 μm diameter orifice in a 2.5-μm-thick nickel foil that was spot welded into a small counter bore in the center of the bottom grounded electrode of the reactor. For IED measurements, the ions that pass through the orifice are accelerated and focused into a 45° electrostatic energy selector. After being selected according to their energy, the ions enter a quadrupole rf mass spectrometer where they are selected according to their mass-to-charge ratio and detected with an electron multiplier. Ions with kinetic energies in excess of 2 eV were recorded. The resolution of the electrostatic analyzer was fixed at a value of 1 eV, full width at half maximum, and the uncertainty of the energy scale is estimated to be less than ±1 eV.

For pulsed operation of the reactor, the rf power to the induction coil was supplied by an rf amplifier with its input connected to a wave form synthesizer operating at 13.56 MHz. A master gate pulse generator with a variable pulse repetition rate and duty cycle was used to gate the rf output and synchronize all time-resolved measurements. Time-resolved IED measurements were made by gating the digital ion counting pulses from the electron multiplier. The gating pulse, which could be varied in width, was synchronized to the master gate pulse generator through a variable digital delay generator.

Electrical measurements of the current and voltage to the induction coil were made with home-built probes that were calibrated against commercially available probes. The transient voltage and current signals were recorded with a digital oscilloscope that was operated in the envelope mode so that only the maximum amplitudes of the rf current and voltage

[a]Electronic mail: misakian@eeel.nist.gov

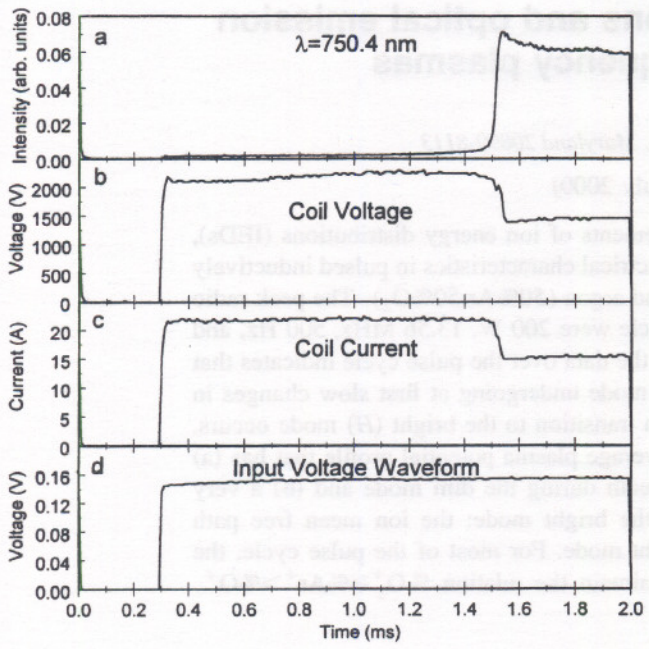

FIG. 1. Recordings of (a) the light emission for the 750.4 nm $4s'[\frac{1}{2}]^\circ - 4p'[1/2]$ transition in argon, (b) coil voltage, (c) coil current, and (d) input voltage.

were recorded. For most of the results reported here, the pulse repetition rate was 500 Hz with a duty cycle of 85% (0.3 ms rf off time), the peak power was 200 W,[13] and the gas was a 50% Ar:50% O_2 mixture. The flow rate for each gas was 5 sccm and the pressure was maintained at 2.67 Pa (20 mTorr) by a variable conductance gate valve between the pump and GEC cell. The IED results were obtained during a time window 0.1 ms wide that was advanced in 0.1 ms or larger steps over the 2 ms period of the pulse cycle. The dwell time at each energy of the IED was typically 100 ms.

It should be noted that while the electrical and light emission data are recorded with insignificant time delay, the IED results are "slower" because of the time to record an IED. In addition, there is a delay in the recording because of the time-of-flight (TOF) of the ions from the GEC cell to the detector in the mass spectrometer (~0.15 ms).

III. EXPERIMENTAL RESULTS

As noted in Sec. I an inductively coupled plasma can exist in two states or modes. When in the dim or *E* mode, the character of the plasma is predominantly that of a capacitively coupled discharge, while during the bright or *H* mode, the character is predominantly that of an inductively coupled discharge.[3,4] This section presents the results of time-resolved measurements of the characteristics of light emission and IEDs (e.g., IED width, peak kinetic energy, relative abundances of different ion species, flux intensities) as part of a process to determine what is taking place in the plasma as a function of time, beginning in the dim mode and advancing to the bright mode. Section IV provides our interpretation of the data as it relates to processes in the plasma.

Figure 1 shows the time sequence of the voltage and current envelopes of the 13.56 MHz rf energy applied to the

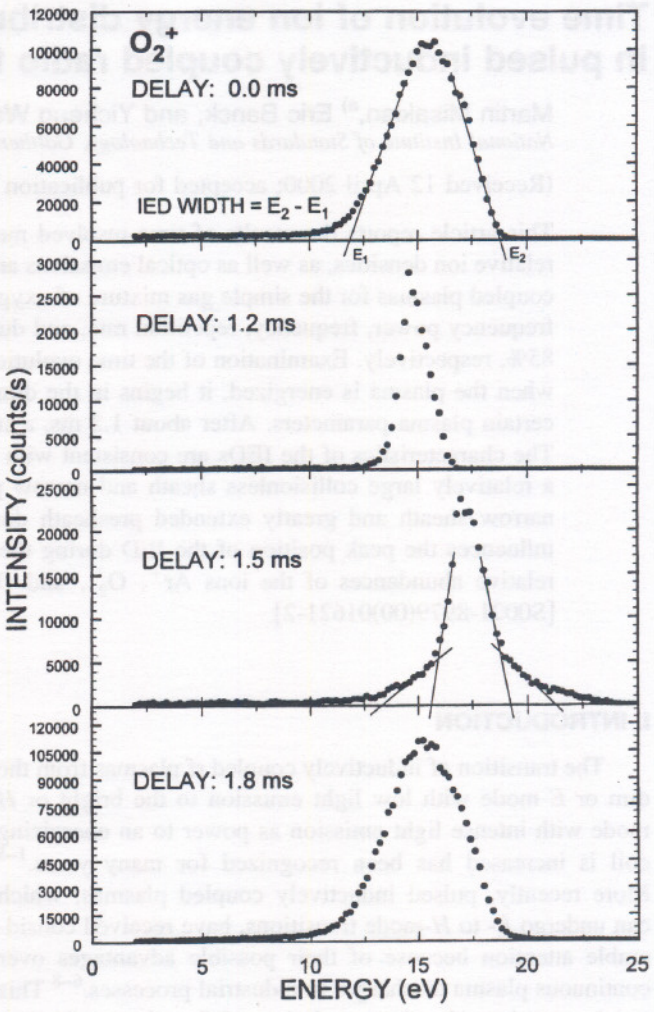

FIG. 2. Examples of O_2^+ IEDs for different time delays during the bright (0 and 1.8 ms delay) and dim (1.2 ms delay) modes. The IED for the 1.5 ms delay likely consists of two IEDs, one from each mode, that are superimposed. The IED width is determined graphically as shown in the top frame.

planar induction coil. Figure 1 also shows the corresponding light emission at 750.4 nm for the $4s'[\frac{1}{2}]^\circ - 4p'[1/2]$ transition in argon. The light emission and electrical data in Fig. 1 indicate that the discharge ignites in the dim mode when the rf energy is turned on at $t=0.3$ ms, and remains in the dim mode until $t\approx 1.5$ ms, at which time the plasma undergoes a transition to the bright mode (~1.5–2 ms). The *E* mode is characterized by a higher coil voltage and current than in the *H* mode. Although the voltage and current to the coil are higher in the *E* mode, the corresponding power deposited in the plasma is much lower as suggested by the light intensity results. The lower deposition of power is correlated with increased reflected power from the matching network that couples the rf source to the induction coil and increased power loss in the coil (I^2R_{eff}), where I is the current and R_{eff} is the effective resistance. The time duration in the dim and bright modes, as indicated by the light emission and voltage/current results, was sufficiently long to permit time-resolved measurements of IEDs during both modes of the discharge as described later.

Figure 2 shows examples of O_2^+ IEDs recorded follow-

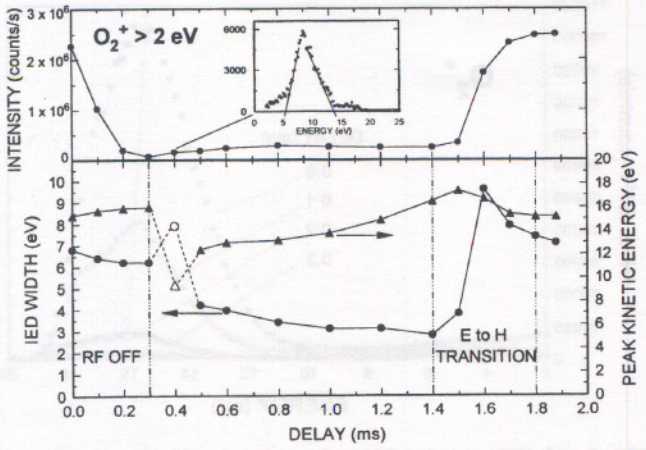

FIG. 3. The peak kinetic energy, IED width, and intensity of O_2^+ as a function of delay time.

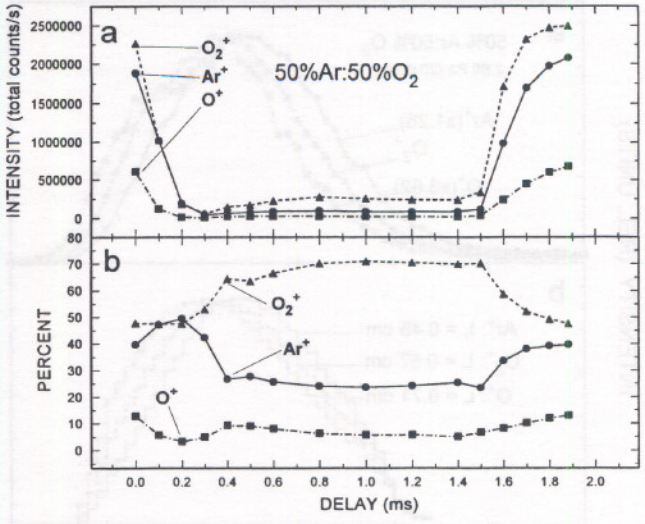

FIG. 4. Abundances of ions with kinetic energy >2 eV. (a) The abundances of the three ion species according to their intensities (counts/s). (b) The relative abundances expressed in terms of their percentage of the total intensity.

ing several delays after the plasma is turned off at $t=0$ and subsequently reignited at $t=0.3$ ms. Similar IEDs are observed for Ar^+ and O^+, but the O^+ data is more noisy because of lower flux intensity (counts/s). Although the rf power has been turned off at $t=0$, the O_2^+ IED for zero delay corresponds to about 0.15 ms earlier in time before the plasma is extinguished because of the previously noted ion TOF from the GEC reactor to the detector in the mass spectrometer. In general, the width of the IEDs, i.e., E_2-E_1 in Fig. 2, becomes more narrow and the intensity becomes much lower during the dim mode.

Figure 3 supplements the information in Fig. 2 by showing the values of the peak O_2^+ IED kinetic energy, IED widths, and intensity for most of the pulse period as a function of delay time. The open data points for the 0.4 ms delay (Fig. 3, lower frame) represent approximate values of the width and peak kinetic energy because of experimental uncertainties in the values of these parameters as can be seen in the inset in the upper frame of Fig. 3. Similar results are seen for the Ar^+ and O^+ data. The IED width plotted in Fig. 3 for the 1.5 ms delay is actually for the narrower of two IED widths that are superimposed at 1.5 ms (see Fig. 2). During the transition to the bright mode, the IED width and maximum kinetic energy "overshoot" the more typical values observed in the bright mode. A similar overshoot occurs at about the same time for the argon light emission (Fig. 1).

In the upper frame of Fig. 3, it can be seen that the intensity of the O_2^+ ion flux changes dramatically as the plasma undergoes a transition between the two modes. For purposes of comparison, the total flux intensity for each ion species as a function of time delay is shown in Fig. 4(a). For each delay and ion species, the total flux intensity was determined by summing the counts/s in the energy bins of the IED (0.1 eV wide). The relative abundances of Ar^+, O_2^+, and O^+ as a function of delay time are plotted in Fig. 4(b). Throughout the pulse cycle, ions with kinetic energies greater than 2 eV maintain the relation $\%O_2^+ \geq \%Ar^+ > \%O^+$.

During the current study, there was no provision for direct measurements of the average plasma potential or potential profile, which are parameters of some interest. However, earlier measurements of Ar^+ IEDs during the bright mode of an Ar plasma have yielded information regarding these parameters via model calculations.[14] Comparisons were made between Ar^+ IEDs obtained from Ar and Ar/O_2 plasmas to see if similar information could be inferred for the gas mixture case. Figure 5 compares an Ar^+ IED at zero delay from the Ar/O_2 plasma with an Ar^+ IED recorded several days later from a pure argon plasma for the same time delay and plasma conditions (rf frequency, peak power, pressure, and duty cycle). The peak heights have been made equal for the comparison. The earlier model calculations indicate that the Ar^+ IED recorded from the pure argon plasma during the bright mode is formed from ions that come mainly from an extended presheath region that reaches nearly to the center of the bulk plasma.[14] The near coincidence of the IEDs in Fig. 5 suggest that the average plasma potential profile for the gas mixture is very similar to the Ar plasma and the consequences of this observation are considered in more detail in Sec. IV.

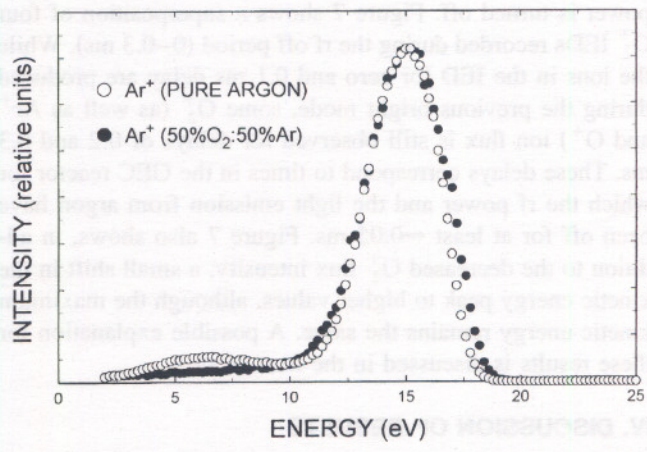

FIG. 5. Comparison of Ar^+ IEDs from a pure argon plasma (○) and from its 50% mixture with oxygen (●) for zero time delay.

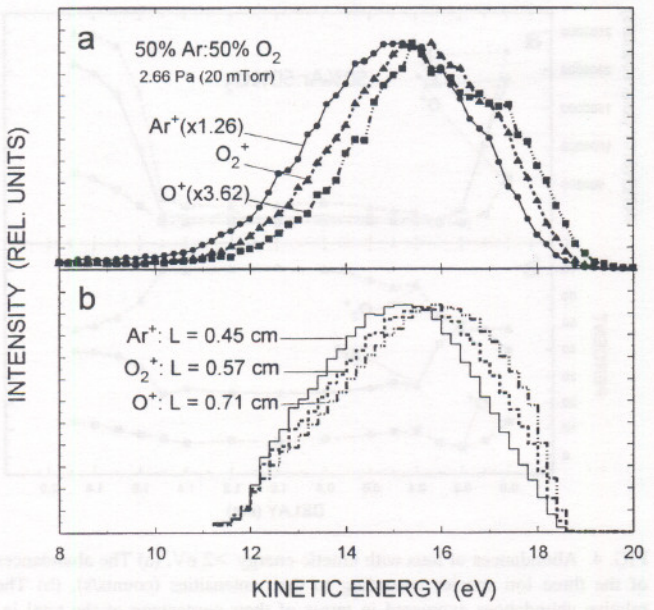

FIG. 6. Measured and calculated IEDs for zero time delay. (a) IEDs for O_2^+, Ar^+, and O^+ adjusted to have the same peak height. (b) Calculated IEDs showing the influence of mean free path, L, on the position of peak kinetic energy.

During the bright mode, it was observed that the peak kinetic energies of the different ion species did not coincide. For example, this can be seen in the recordings of IEDs for Ar^+, O_2^+, and O^+ for zero time delay in Fig. 6(a). The peak heights of the three IEDs have been made equal for the comparison. The results of model calculations for three IEDs with masses corresponding to Ar^+, O_2^+, and O^+, assuming (average) mean free paths of 0.45, 0.57, and 0.71 cm, respectively, are shown in Fig. 6(b). The model calculations are discussed in the next section and were made possible by insights gained from the IED comparison discussed earlier (Fig. 5). While the calculated IED for Ar^+ has been made to agree with the experimental IED, those for O_2^+ and O^+, using the same model, are too wide relative to the experimental results. In addition, the IED for O^+ exhibits some structure near its peak.

The final experimental result that is presented is a closer examination of the way the IED signal decays after the rf power is turned off. Figure 7 shows a superposition of four O_2^+ IEDs recorded during the rf off period (0–0.3 ms). While the ions in the IED for zero and 0.1 ms delay are produced during the previous bright mode, some O_2^+ (as well as Ar^+ and O^+) ion flux is still observed for delays of 0.2 and 0.3 ms. These delays correspond to times in the GEC reactor for which the rf power and the light emission from argon have been off for at least ≈0.05 ms. Figure 7 also shows, in addition to the decreased O_2^+ flux intensity, a small shift in the kinetic energy peak to higher values, although the maximum kinetic energy remains the same. A possible explanation for these results is discussed in the next section.

IV. DISCUSSION OF RESULTS

With the exception of some calculated results at the end of this section pertaining to IEDs in the dim mode, the results presented in the previous section are now discussed in nearly the same order as they were presented earlier.

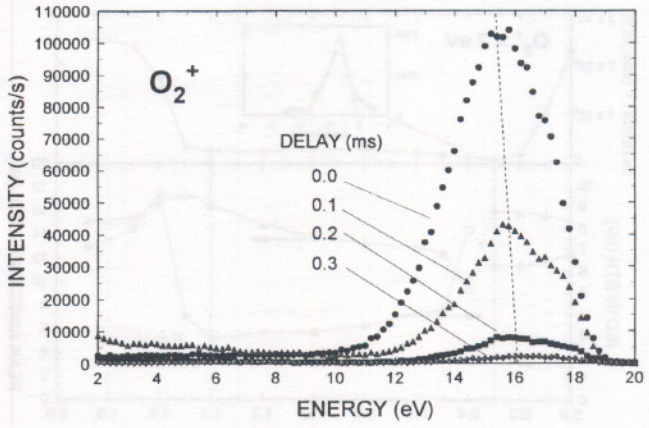

FIG. 7. O_2^+ IEDs recorded during the period that the rf energy has been turned off.

Figures 1–3 indicate that conditions during the dim mode are not static, but rather characterized by slowly increasing light emission, slowing increasing IED peak and maximum kinetic energies, and slowly decreasing IED widths. The relatively small difference in the IED kinetic energies in the two modes suggests that the average plasma potential does not change greatly after transitions between the two modes, e.g., the peak kinetic energy differs by less than about 5 eV between the two modes. This observation and the fact that the ion current, J, is smaller by over an order of magnitude [Figs. 3 and 4(a)] in the dim mode is consistent with, from the Child–Langmuir law[15]

$$J = C\frac{V^{3/2}}{s^2}, \tag{1}$$

a much larger sheath width, s, between the bulk plasma and ground electrode during the dim mode. In Eq. (1), C is a constant and V is the sheath potential. A large sheath width combined with a relatively small plasma/sheath potential (and modulation amplitude) could explain the more narrow IEDs observed in the dim mode (Figs. 2 and 3), i.e., because of longer TOFs for ions crossing the sheath, the IEDs tend to become more monoenergetic, approaching the value of the average plasma potential. This interpretation of the data during the dim mode is further supported by the fact that the widths of the IEDs for $Ar^+(W_{Ar^+})$, $O_2^+(W_{O_2^+})$, and $O^+(W_{O^+})$ maintain the relation $W_{Ar^+} < W_{O_2^+} < W_{O^+}$ (data not shown). Because the heavier ions have longer TOFs across the sheath, it is expected that their IEDs again would be more narrow. The widening of the sheath width and the shape of the average potential profile in the plasma during the dim and bright modes are discussed further at the end of this section.

The small difference in the average plasma potential between the two modes of the Ar/O_2 plasma is in sharp contrast to the difference observed in a 50% Ar:50%CF_4 plasma under similar experimental conditions.[11] That is, the experimental conditions that could be controlled (apparatus, pressure, peak power, pulse repetition rate, etc.) were the same

except for the duty cycle, which was 95% (0.1 ms rf off time). The change in plasma potential after the transition to the dim mode was roughly +25 V and the reduced TOF of ions traversing the sheath led to IEDs that were much wider and bimodal in character because of rf modulation.[11]

The brief overshoot observed in the argon light emission results (Fig. 1) and O_2^+ width data (Fig. 3) during the transition to the bright mode near 1.6 ms is also accompanied by an overshoot in the maximum kinetic energy for all ion species. An indication of the higher maximum kinetic energy is seen in Fig. 2 for the 1.5 ms delay, which as already noted, shows a superposition of two IEDs. That is, the plasma during the 1.5 ms measurement appears to be moving back and forth between the two modes of the discharge and the ion sampling system is capturing IEDs from the end of the dim mode and the beginning of the following bright mode. Under somewhat different experimental conditions in a pulsed argon plasma (e.g., 200 Hz repetition rate, 30% duty cycle (1.5 ms pulse-on), 1.33 Pa (5 mTorr), aluminum chamber, lower power), a similar overshoot in the plasma *density* has been observed.[16] However, an overshoot in the plasma density does not appear to take place for our conditions because no overshoot in the ion current is observed (Figs. 3 and 4).

The data in Fig. 4 indicate that the ion flux intensities for O_2^+, Ar^+, and O^+ are larger by factors of about 10, 25, and 34, respectively, comparing intensities in the dim mode (1.0 ms delay) and bright mode (1.88 ms delay), i.e., the ion species with the lower intensities undergo greater relative increases following transition to the bright mode. As already noted, Fig. 4 shows that throughout the pulse cycle the ion abundances have the relation $\%O_2^+ \geqslant \%Ar^+ > \%O^+$. The relative number of positive ions for each ion species correlates well with the its ionization threshold for direct ionization following electron impact, i.e.,

(a) $e + O_2 \rightarrow O_2^+ + 2e \quad (\geqslant 12.1\ \text{eV})$
(b) $e + O_2 \rightarrow O^+ + O^- + e \quad (\geqslant 17.3\ \text{eV})$
(c) $e + O_2 \rightarrow O^+ + O + 2e \quad (\geqslant 18.7\ \text{eV})$
(d) $e + Ar \rightarrow Ar^+ + 2e \quad (\geqslant 15.8\ \text{eV}).$

While the cross section for ionization of Ar [process (d)] quickly exceeds that for O_2^+ [process (a)] as the electron energy increases above 15.8 eV,[17,18] the data suggest that the convolution of the electron energy distribution over the O_2 and Ar cross sections for ionization favors process (a). The low abundance of O^+ from processes (b) and (c) is understandable in terms of their higher thresholds and much smaller ionization cross sections compared with the production of O_2^+.[19]

The two step ionization process for argon via an argon metastable state Ar* ($^3P_2, ^3P_0$),

$$e + Ar \rightarrow Ar^* + e$$

$$e + Ar^* \rightarrow Ar^+ + 2e,$$

which has a large cross section for the second step,[20] apparently is not frequent enough to alter the relative abundances. We note that collisions of Ar* with ground state O_2 will not ionize O_2 because of insufficient metastable energy.

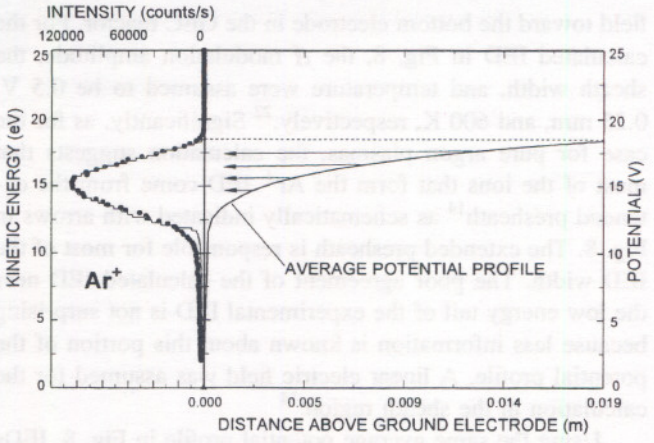

FIG. 8. The average potential profile in the right frame is used to calculate the Ar^+ IED as a histogram in the left frame for zero time delay. The measured argon IED is also shown in the left frame. Ions that contribute to the IED, indicated schematically with arrows, come mainly from the presheath that extends deep into the bulk plasma.

The earlier conclusion regarding the relative abundances of Ar^+ and O_2^+ rests in part on the assumption that the ions sampled by the mass spectrometer have uniform density profiles in the plasma. This point is discussed further later.

The similarity in the bright mode of the Ar^+ IEDs from pure Ar and 50% Ar:50% O_2 plasmas in Fig. 5 suggests that a similar average potential profile exists in the bulk plasma and sheath regions for the Ar/O_2 plasma during the bright mode and may to a great extent control the shape and energies of the IEDs for all ion species. This possibility was explored by first fitting a calculated IED to the Ar^+ IED from the Ar/O_2 plasma shown in Fig. 5. Figure 8 shows an average potential profile with a "presheath" that extends to nearly the center of the bulk plasma in the GEC reactor, very similar to ones used for calculating IEDs from pulsed (pure) argon plasmas during the bright mode.[14,21] The calculated Ar^+ IED using this profile and methods described in detail elsewhere[14] is shown as a histogram to the left of the average potential profile in Fig. 8 with the experimental Ar^+ IED. The potential profile was adjusted slightly from the pure argon case to fit the experimental Ar^+ IED obtained from the gas mixture.

Numerous simplifying approximations are made in the model calculation,[14] including uniform charge densities throughout most of the plasma, all ions that reach the grounded electrode begin with thermal energies, ions come under the influence of the electric field at a uniform rate for different phases of the field and from a range of starting points, X_0, extending to 0.019 m above the grounded electrode. It is assumed that the probability of an ion reaching the grounded electrode is proportional to

$$WT = \exp\left(-\frac{X_0}{L}\right)\exp\left(-\frac{m v_T^2}{2kT}\right), \tag{2}$$

where the first exponential is the mean free path (mfp) distribution with an average mfp value of L, and the second exponential is (within a constant) the Maxwellian velocity distribution, with k equal to the Boltzmann constant, m is the ion mass, T is the absolute temperature, and v_T is the thermal velocity of the ion as it begins its movement in the electric

field toward the bottom electrode in the GEC reactor. For the calculated IED in Fig. 8, the rf modulation amplitude, the sheath width, and temperature were assumed to be 0.5 V, 0.25 mm, and 600 K, respectively.[22] Significantly, as for the case for pure argon plasmas, the calculation suggests that most of the ions that form the Ar^+ IED come from the extended presheath[14] as schematically indicated with arrows in Fig. 8. The extended presheath is responsible for most of the IED width. The poor agreement of the calculated IED near the low energy tail of the experimental IED is not surprising because less information is known about this portion of the potential profile. A linear electric field was assumed for the calculation in the sheath region.[14]

Using the same average potential profile in Fig. 8, IEDs were also calculated for O_2^+ and O^+ and are shown as histograms with the calculated Ar^+ IED in Fig. 6(b). The calculated IEDs were made to match the peak kinetic energies of the corresponding experimental IEDs in Fig. 6(a) by using the average mfp as a fitting parameter, i.e., $L=0.45$, 0.57, and 0.71 cm for Ar^+, O_2^+ and O^+, respectively. The peak heights of the calculated distributions were made the same to better compare with the experimental results in Fig. 6(a). The calculated fit for Ar^+ is quite good (Fig. 8). The calculated fit for the O_2^+ IED is good for much of the main portion of experimental IED, but has an excess of-ions on the low energy side of the distribution. The calculated fit for the O^+ IED is only fair with too many ions predicted on the low energy side of the distribution. While the agreement between the calculated and experimental IEDs ranges from very good to fair, the calculated results in Fig. 6(b) suggest that the relative peak kinetic energy positions of the different IEDs may be explained mainly by differences in the mean free paths of the different ion species. We note that the mfp used as fitting parameters for the Ar^+ and O_2^+ IEDs are not unrealistic. Approximate calculations (not shown) indicate that both mean free paths are consistent with the charge exchange cross sections of these ions with their respective neutral gases.[23,24] A similar rough consistency check of the mfp used for the O^+ IED appears to be limited by the available cross-section data on collision processes for this ion. The charge exchange cross section for O^+ with O_2 is over an order of magnitude smaller than for O_2^+.[25,26] Considering only charge exchange collisions for O^+ leads to a mfp in excess of 10 cm, which is physically unreasonable in the present case.

It should be realized that the maximum kinetic energy of the O^+ IED in Fig. 6(a), which seems to be greater than for Ar^+ and O_2^+, is an artifact caused by the multiplication of the O^+ IED intensity. Thus, it appears that any kinetic energy acquired by O^+ during the dissociative ionization process[27] has been transformed to thermal energies by collision processes before contributing to the IED.

The reason for structure near the peak of the O^+ IED in Fig. 6(a) is not clear. A possible explanation is that the density of O^+ in the plasma is not uniform during the bright mode (as was assumed in the calculation) and has a downward dip in the interior of the plasma. The downward dip might also cause a small dip in the plasma potential profile in the bulk plasma. Such a dip in the plasma potential profile would in principle affect the shapes of the IEDs for all ion species, with the lightest ion, O^+, most affected. That is, because heavier ions have longer TOFs, small structures in the potential profile would be "averaged out" in the IED due to the rf modulation. Some evidence for this interpretation of the data is given in the IEDs for Ar^+ and O_2^+ during the bright mode. For example, a trace of structure appears to occur near the peak kinetic energy of O_2^+ for the 1.8 ms delay (Fig. 2) and 1.88 ms (data not shown), although the structure for zero time delay (Fig. 2) is questionable. The heaviest ion species, Ar^+, did not exhibit discernible structure in any of its IEDs. The O^+ density may also be less near the edge of the bulk plasma, which would explain their fewer numbers along the low energy side of the IED when compared to the calculated IED (see potential profile in Fig. 8).

The persistence of the IEDs after the rf energy has been turned off (Fig. 7, 0.2 and 0.3 ms delays) is very interesting. Although the IED intensity is greatly reduced, the similarity of the IED shapes to those observed during the bright mode indicates that the average potential profile in the bright mode also tends to persist. The data suggest that the electric field that existed during the bright mode is quickly replaced by an ambipolar field that extends deep into the bulk plasma. This observation is similar to one reported for a pulsed Ar/CF_4 plasma.[11] Because the maximum kinetic energy of the IEDs does not change (Fig. 7), the data suggests that the maximum potential does not change. The narrowing of the IEDs would be consistent with an increase in the sheath width, i.e., the residual plasma shrinks in volume. A similar persistence of the plasma density in a pulsed argon discharge following extinction of the rf energy has been directly measured, although for somewhat different experimental conditions.[16]

Earlier, we suggested that the narrowing of the IEDs during the dim mode might be explained by a large increase in the sheath width compared to that in the bright mode. The plausibility of this interpretation was examined by performing model calculations of IEDs corresponding to O_2^+ IEDs measured during the dim mode for delays of 0.6 and 1.4 ms. In the model calculations, using methods described in Ref. 14, the average potential profile with an extended presheath that reaches to near the center of the bulk plasma (Fig. 8) is replaced with average potential profiles that are flat in most of the plasma but with much wider sheath/presheath regions as shown in Fig. 9. We assume that the electric field in the sheath/short presheath region is linear and has an average potential profile of the form used by Fivaz *et al.*[28]

$$V_F(x) = -(V_s - d)\left(\frac{x - x_s}{x_s}\right)^2 + d\frac{(x - x_s)}{x_s} + V_s, \quad (3)$$

where x is the distance above the grounded electrode, V_s is the sheath potential, x_s is the sheath width, and the parameter d is associated with the electric field in the presheath region.[28]

The inset of Fig. 9 shows the results of two model calculations. To obtain the calculated O_2^+ IED corresponding to a delay of 0.6 ms, the values of V_s, x_s, d, L, and T were assumed to be 12.4 V, 3.5 mm, 5 V, 0.57 cm, and 600 K, respectively. The amplitude of rf modulation was taken to be 12.4 V and it was assumed that O_2^+ ions contributing to the IED came from a narrow range of distances near the edge of

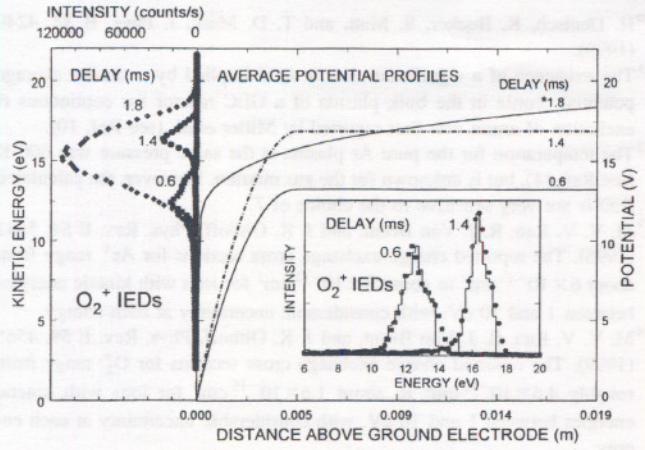

FIG. 9. Assumed average potential profiles during the dim and bright modes and corresponding calculated and measured O_2^+ IEDs. The potential profiles assumed for the 0.6 and 1.4 ms calculations in the inset show a zero electric field in the bulk plasma and a relatively wide sheath region (dim mode) compared to the profile corresponding to the*1.8 ms delay which has a presheath that extends into the interior of the bulk plasma (bright mode). The*1.8 ms profile is actually the same as the profile for zero delay shown in Fig. 8. Little difference is expected between the two profiles.

the bulk plasma, 2.9–4.5 mm above the grounded electrode. The calculated IED corresponding to the more narrow 1.4 ms delayed IED was obtained with V_s, x_s, d, L, and T assumed to be 16.4 V, 4 mm, 5 V, 0.57 cm, and 600 K, respectively, and a rf modulation amplitude of 11 V. Ions that contributed to the calculated IED were assumed to come from a narrow range of distances 3.6–4.4 mm above the grounded electrode again near the edge of the bulk plasma. The relative positions and shapes of O_2^+ IEDs corresponding to delays of 0.6, 1.4 (dim mode), and 1.8 ms (bright mode) are shown in the left panel of Fig. 9. The potential profile associated with the 1.8 ms delay is actually that used for calculating the zero delayed Ar^+ IED (Fig. 8). The two potential profiles (zero delay and 1.8 ms delay) will not differ greatly because of the similarity of the Ar^+ IEDs for the two cases.

The fits of the calculated IEDs in Fig. 9 are not bad considering that no information is available on the actual potential profiles and many assumptions were made regarding the other parameters used in the calculations. However, the process of determining features of the average potential profile in the dim mode via a fitting process of measured IEDs cannot be uniquely done without further information[14] and thus the calculated results in Fig. 9 must be regarded as only addressing the question of plausibility. In that regard, it is noteworthy that the assumptions that go into the calculations are not physically unrealistic and the reasoning given earlier regarding the narrowing of the IEDs during the dim mode may be qualitatively correct.

We note that because the mfp is comparable to the sheath width during the dim mode, there will be few collisions and the influence of the mfp on the peak kinetic energy will be negligible (compared to the bright mode). This has been confirmed by calculation and is consistent with the fact that the peak kinetic energies of all three ion species coincide as a function of delay time during the dim mode (data not shown).

V. SUMMARY AND CONCLUSIONS

Through examination and analyses of IEDs, light intensity, and electrical measurements, for our conditions a number of observations can be made. When the rf power is turned on, the plasma ignites in the dim mode and undergoes slow changes in its properties before it suddenly changes to the bright mode. The duration of the bright mode is about 42% of the dim mode.

The IED results for the two modes of plasma discharge are consistent with:

(a) a flat potential profile (i.e., zero electric field) in the bulk plasma during the dim mode and ions that form the IEDs come predominantly from the edge of the bulk plasma, acquiring their kinetic energy while traversing a relatively wide sheath/narrow presheath; because of the relatively wide sheath and low amplitude of rf modulation of the average potential profile, the IEDs are narrow and do not exhibit bimodal structure often seen during capacitively coupled plasmas, and

(b) an average potential profile that has an extended presheath reaching nearly to the center of the bulk plasma during the bright mode. Ions that form the IEDs during the bright mode come from a range of distances reaching into the interior of the plasma, and most of the IED is composed of ions from the extended presheath.

If the above interpretation of the data is correct and there are parallels in other gas mixtures, the difference in where the ions forming the IED come from, i.e., from the edge versus the interior of the bulk plasma, may have implications when pulsed inductively coupled plasmas are considered for plasma processing. For example, if the density profile of ions is not uniform throughout the plasma and there are multiple ion species, there could be differences in the predominant ion or mix of ions in the flux impacting a target wafer, depending on the mode of the plasma excitation.

During the bright mode, the peak positions of the IEDs for the different ion species appear to be significantly influenced by the length of their mean free paths. During the dim mode, the peak kinetic energies of all ion species coincide and the influence of the mfp is negligible.

The relative abundances of the different ion species determined from the IED data (kinetic energy >2 eV) maintain the relation $\%O_2^+ \geqslant \%Ar^+ > \%O^+$, although the relation between O_2^+ and Ar^+ may be affected if there exist spatial nonuniformities in their respective densities.

The persistence of an ion flux after the rf power has been turned off for the 50% mixture of argon with oxygen and for pure argon is an interesting phenomenon that has been reported previously for the gas mixture 50%Ar:50%CF_4.

[1] K. A. MacKinnon, Philos. Mag. **8**, 605 (1929).
[2] K. Chandrakar, Journal of Physics D: Applied Physics **11**, 1809 (1978).
[3] U. Kortshagen, N. D. Gibson, and J. E. Lawler, Journal of Physics D: Applied Physics **29**, 1224 (1996).
[4] I. M. El-Fayoumi, I. R. Jones, and M. M. Turner, Journal of Physics D: Applied Physics **31**, 3082 (1998).
[5] K. Suzuki, K. Nakamura, H. Ohkubo, and H. Sugai, Plasma Sources Sci. Technol. **7**, 13 (1998).
[6] S. Samukawa, Jpn. J. Appl. Phys., Part 1 **33**, 2133 (1994).
[7] S. Samukawa and H. Ohtake, J. Vac. Sci. Technol. A **14**, 3049 (1996).

[8] G. A. Hebner and C. B. Fleddermann, J. Appl. Phys. **82**, 2814 (1997).
[9] P. J. Hargis, Jr. *et al.*, Rev. Sci. Instrum. **65**, 140 (1994).
[10] P. A. Miller, G. A. Hebner, K. E. Greenberg, P. D. Pochan, and B. P. Aragon, J. Res. Natl. Inst. Stand. Technol. **100**, 427 (1995).
[11] Y. Wang, E. C. Benck, M. Misakian, M. Edamura, and J. K. Olthoff, J. Appl. Phys. **87**, 2114 (2000).
[12] J. K. Olthoff and Y. Wang, J. Vac. Sci. Technol. A **17**, 1552 (1999).
[13] Because the plasma and the corresponding impedance continually changes during the pulsed excitation of the plasma, it is not possible for the matching network coupling the rf energy to the coil to be continually optimized. For the IED measurements reported in this article, the matching network was optimized for continuous excitation and the rf power value indicated is for the net power to the matching network driving the coil under continuous excitation.
[14] M. Misakian and Y. Wang, J. Appl. Phys. **87**, 3646 (2000).
[15] M. A. Lieberman and A. J. Lichtenberg, *Principles of Plasma Discharges and Materials Processing* (Wiley, New York, 1994).
[16] S. Ashida, M. R. Shim, and M. A. Lieberman, J. Vac. Sci. Technol. A **14**, 391 (1996).
[17] L. G. Christophorou, *Atomic and Molecular Radiation Physics* (Wiley-Interscience, New York, 1971).
[18] E. Krishnakumar and S. K. Srivastava, Int. J. Mass Spectrom. Ion Processes **113**, 1 (1992).
[19] Y. Itikawa *et al.*, J. Phys. Chem. Ref. Data **18**, 23 (1989).
[20] H. Deutsch, K. Becker, S. Matt, and T. D. Märk, J. Phys. B **32**, 4249 (1999).
[21] The existence of a significant electric field implied by a similar average potential profile in the bulk plasma of a GEC reactor for continuous rf excitation of argon was first reported by Miller *et al.* (see Ref. 10).
[22] The temperature for the pure Ar plasma at the same pressure was 600 K (see Ref. 14), but is unknown for the gas mixture. However, the calculated IED is not very sensitive to the choice of T.
[23] M. V. V. Rao, R. J. Van Brunt, and J. K. Olthoff, Phys. Rev. E **54**, 5641 (1996). The reported charge exchange cross sections for Ar^+ range from about $6\times10^{-15}\,cm^2$ to about $3\times10^{-15}\,cm^2$ for ions with kinetic energies between 1 and 10 eV, with considerable uncertainty at each energy.
[24] M. V. V. Rao, R. J. Van Brunt, and J. K. Olthoff, Phys. Rev. E **59**, 4565 (1999). The reported charge exchange cross sections for O_2^+ range from roughly $4.6\times10^{-15}\,cm^2$ to about $1.6\times10^{-15}\,cm^2$ for ions with kinetic energies between 1 and 10 eV, with considerable uncertainty at each energy.
[25] P. H. G. Dickinson and J. Sayers, Proc. Phys. Soc. **76**, 137 (1960).
[26] P. H. Batey, G. R. Court and J. Sayers, Planet. Space Sci. **13**, 911 (1965).
[27] R. J. Van Brunt, G. M. Lawrence, L. J. Kieffer, and J. M. Slater, J. Chem. Phys. **61**, 2032 (1974).
[28] M. Fivaz, S. Brunner, W. Schwarzenbach, A. A. Howling, and Ch. Hollenstein, Plasma Sources Sci. Technol. **4**, 373 (1995).